Cell Reports

Article

Interleukin-17 affects synaptic plasticity and cognition in an experimental model of multiple sclerosis

Graphical abstract

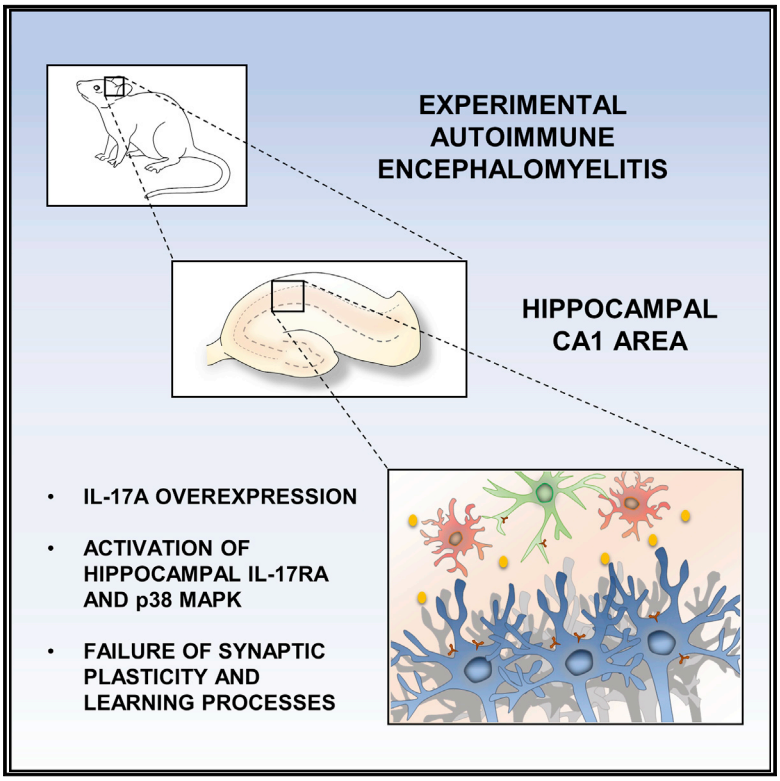

Highlights

- Hippocampal neurons express IL-17RA both under control conditions and during EAE
- IL-17A dose-dependently blocks LTP via the activation of IL-17RA and p38 MAPK
- Hippocampal IL-17A overexpression and synaptic dysfunction both occur during EAE
- The lack of IL-17A ameliorates EAE-related cognitive deficits

Authors

Massimiliano Di Filippo, Andrea Mancini, Laura Bellingacci, ..., Maria Teresa Viscomi, Luigina Romani, Paolo Calabresi

Correspondence

massimiliano.difilippo@unipg.it

In brief

In this study, Di Filippo et al. investigate the pathogenesis of hippocampal synaptopathy in experimental autoimmune encephalomyelitis, highlighting an IL-17A-centered neuro-immune cross-talk. Besides its well-known immunopathogenic roles, the IL-17 axis might be directly involved in the modulation of synaptic plasticity and cognition, with potential therapeutic implications for people with multiple sclerosis.

Di Filippo et al., 2021, Cell Reports *37*, 110094
December 7, 2021
https://doi.org/10.1016/j.celrep.2021.110094

CellPress

Cell Reports

CellPress
OPEN ACCESS

Article

Interleukin-17 affects synaptic plasticity and cognition in an experimental model of multiple sclerosis

Massimiliano Di Filippo,[1,11,*] Andrea Mancini,[1,10] Laura Bellingacci,[1,10] Lorenzo Gaetani,[1] Petra Mazzocchetti,[1] Teresa Zelante,[2] Livia La Barbera,[3] Antonella De Luca,[2] Michela Tantucci,[1] Alessandro Tozzi,[4] Valentina Durante,[1] Miriam Sciaccaluga,[1] Alfredo Megaro,[1] Davide Chiasserini,[4] Nicola Salvadori,[1] Viviana Lisetti,[1] Emilio Portaccio,[5] Cinzia Costa,[1] Paola Sarchielli,[1] Maria Pia Amato,[5,6] Lucilla Parnetti,[1] Maria Teresa Viscomi,[7] Luigina Romani,[2] and Paolo Calabresi[8,9]

[1]Section of Neurology, Department of Medicine and Surgery, University of Perugia, Perugia, Italy
[2]Section of Pathology, Department of Medicine and Surgery, University of Perugia, Perugia, Italy
[3]Unit of Molecular Neurosciences, Department of Medicine, University Campus-Biomedico, Rome, Italy
[4]Section of Physiology and Biochemistry, Department of Medicine and Surgery, University of Perugia, Perugia, Italy
[5]Department of NEUROFARBA, University of Florence, Florence, Italy
[6]IRCCS Fondazione Don Carlo Gnocchi, Florence, Italy
[7]Section of Histology and Embryology, Department of Life Science and Public Health, Università Cattolica del Sacro Cuore, Rome, Italy
[8]Neurology, Fondazione Policlinico Universitario Agostino Gemelli, IRCCS, Rome, Italy
[9]Section of Neurology, Department of Neuroscience, Università Cattolica del Sacro Cuore, Rome, Italy
[10]These authors contributed equally
[11]Lead contact
*Correspondence: massimiliano.difilippo@unipg.it
https://doi.org/10.1016/j.celrep.2021.110094

SUMMARY

Cognitive impairment (CI) is a disabling concomitant of multiple sclerosis (MS) with a complex and controversial pathogenesis. The cytokine interleukin-17A (IL-17A) is involved in the immune pathogenesis of MS, but its possible effects on synaptic function and cognition are still largely unexplored. In this study, we show that the IL-17A receptor (IL-17RA) is highly expressed by hippocampal neurons in the CA1 area and that exposure to IL-17A dose-dependently disrupts hippocampal long-term potentiation (LTP) through the activation of its receptor and p38 mitogen-activated protein kinase (MAPK). During experimental autoimmune encephalomyelitis (EAE), IL-17A overexpression is paralleled by hippocampal LTP dysfunction. An *in vivo* behavioral analysis shows that visuo-spatial learning abilities are preserved when EAE is induced in mice lacking IL-17A. Overall, this study suggests a key role for the IL-17 axis in the neuro-immune cross-talk occurring in the hippocampal CA1 area and its potential involvement in synaptic dysfunction and MS-related CI.

INTRODUCTION

Multiple sclerosis (MS) is a chronic disease of the central nervous system (CNS) that affects mainly young adults and is pathologically characterized by the presence of inflammation, demyelination, and neuro-axonal damage (Reich et al., 2018). During its course, MS is responsible for accumulating neurological disability due to the involvement, since the earliest phases, of different functional systems, from motor function to cognition (Reich et al., 2018). The presence of cognitive impairment (CI) has been overlooked for a long time in people with MS (DeLuca et al., 2015), but it is now clearly recognized as a frequent and impactful feature of the MS clinical picture, with a significant detrimental effect on many key aspects of daily life, ranging from employability to social relationships and physical independence (DeLuca et al., 2015). The pathogenesis of MS-related cognitive dysfunction is complex and far from being definitely elucidated (Di Filippo et al., 2018), and it seems to rely on a scenario involving different mechanisms (Rocca et al., 2015). The presence of focal white matter demyelinating lesions, together with pathological changes to normally appearing white matter, is thought to play a "disconnecting" effect between brain areas playing crucial cognitive functions (Dineen et al., 2009; Hulst et al., 2015; Preziosa et al., 2016). At the same time, specific roles are also played by focal cortical lesions (Calabrese et al., 2009; Harrison et al., 2015), diffuse cortical atrophy (Calabrese et al., 2009; Steenwijk et al., 2016), and atrophy of strategic cortical and subcortical gray matter structures, such as the hippocampus (Planche et al., 2018), the thalamus (Bergsland et al., 2016), and the cerebellum (Cocozza et al., 2017).

Together with the structural and intertwined damage to the gray and the white matter, it has been hypothesized that a pathogenic role in MS-related cognitive dysfunction may be played by a an immune-mediated disruption of synaptic plasticity (Di

Filippo et al., 2008, 2018), which is the putative synaptic base of memory processes (Nicoll, 2017). Indeed, the main form of synaptic plasticity in the mammalian brain, named long-term potentiation (LTP), has been found to be impaired in experimental models of MS (Di Filippo et al., 2015). Human studies have confirmed a dysfunctional cortical plasticity in cognitively impaired people with MS, as explored with transcranial magnetic stimulation (TMS) (Mori et al., 2012).

The identification of the specific immune molecule and/or cellular mechanism responsible for the observed impairment of synaptic plasticity would allow the design of tailored therapeutic strategies to counteract the MS-related immune-mediated synaptopathy, with implications for the treatment of CI and disease progression. Among the different immune cells with a demonstrated immunopathogenic role during MS, great attention has been recently directed toward T-helper 17 (Th17) lymphocytes, a subtype of pro-inflammatory lymphocytes mainly secreting interleukin-17A (IL-17A) (Moynes et al., 2014), acting on its specific receptor (IL-17R) expressed by immune, glial, and neuronal cells (Moynes et al., 2014). Infiltrating Th17 cells can be detected in the CNS in the earliest phases of experimental (Murphy et al., 2010) and human MS (Tzartos et al., 2008). Although the immunopathogenic role of IL-17A has been clearly demonstrated (Murphy et al., 2010; Tzartos et al., 2008; Zepp et al., 2011), the potential detrimental effects of this cytokine on synaptic function are still largely unexplored. The aim of our study was to investigate the specific effects of IL-17A on the expression of hippocampal synaptic plasticity in order to define its potential role in the pathogenesis of MS-related CI.

RESULTS

IL-17A is able to dose-dependently block hippocampal LTP

In order to investigate the possible effects of IL-17A on hippocampal synaptic plasticity, we performed electrophysiological recordings in the hippocampal CA1 area after exposing control brain slices to increasing IL-17A concentrations (2, 10, and 20 ng/mL). Extracellular CA1 hippocampal field excitatory postsynaptic potential (fEPSP) recordings showed that the exposure of the slices to 2 ng/mL IL-17A did not alter LTP ($p > 0.05$, Figure 1A), whereas higher IL-17A concentrations blocked LTP induction in a dose-dependent manner (10 ng/mL, $p < 0.05$ [Figure 1B]; 20 ng/mL, $p < 0.001$ [Figures 1C and 1D]). The analysis of basal hippocampal synaptic transmission through input/output analysis revealed no differences between control slices and slices exposed to 20 ng/mL IL-17A ($p > 0.05$; Figure 1E), whereas paired-pulse facilitation (PPF) at a 50-ms interval showed a slightly reduced S2/S1 ratio, in the absence of statistical significance ($p > 0.05$; Figure 1F). The alteration of hippocampal LTP after exposure to 20 ng/mL IL-17A was confirmed by also applying the theta-burst stimulation (TBS) induction protocol for LTP ($p < 0.05$; Figure S1A). Patch-clamp recordings of CA1 pyramidal cells demonstrated that 20 ng/mL IL-17A did not alter electric membrane properties with respect to control conditions (Figure S1B) and confirmed its ability to block the induction of LTP ($p < 0.05$; Figure S1C).

The synaptic effects of IL-17A are mediated by the activation of IL-17RA and p38 mitogen-activated protein kinase (MAPK)

The IL-17A-dependent disruption of hippocampal LTP could be related either to the activation of its specific receptor or to a "non-specific" detrimental effect of the cytokine on synapses and neurons. In order to investigate this issue, we performed fEPSP recordings in the hippocampal CA1 region of a genetic murine model lacking the IL-17RA (IL-17RA knockout [KO] mice [IL-17RA$^{-/-}$]). We found that the exposure of brain slices obtained from mice lacking the IL-17RA to 20 ng/mL IL-17A did not influence the induction of synaptic potentiation ($p > 0.05$; Figure 2A), suggesting that IL-17A influences hippocampal synaptic plasticity through the activation of its specific intermembrane receptor. We then investigated the molecular transduction pathway involved in the IL-17A-dependent block of hippocampal LTP. The interaction between IL-17A and its receptor is known to induce the activation of intracellular p38 MAPK (Li et al., 2019; Xu and Cao, 2010; Zepp et al., 2011) that, in turn, is responsible for the different cellular effects exerted by this pro-inflammatory cytokine (Wagner and Nebreda, 2009; Zepp et al., 2011). In order to demonstrate a role of this kinase in the observed IL-17A-mediated-synaptopathy, we performed a western blot analysis of total (p38) and phosphorylated (p-p38) p38 MAPK in hippocampal slices exposed to 20 ng/mL IL-17A or standard artificial cerebrospinal fluid (ACSF) for 1 h, as in the electrophysiological protocol. Interestingly, the phosphorylation of p38 was significantly increased after exposure to 20 ng/mL IL-17A ($p < 0.05$; Figure 2B), with no significant difference in the total level of p38 MAPK between the two groups ($p > 0.05$; Figure 2B). Considering this evidence, we tested if the pharmacological inhibition of p38 MAPK by *in vitro* exposure to SB 202190 was able to counteract the synaptic detrimental effects of IL-17A. Extracellular recordings of hippocampal fEPSP showed that the co-exposure to IL-17A and SB 202190 is able to prevent the IL-17A-dependent disruption of LTP ($p < 0.05$; Figure 2C). Of note, the isolated application of SB 202190 did not alter the physiological induction of hippocampal LTP under control conditions (Ctrl: $n = 5$, 181.72% ± 13.53%; 20 μM SB 202190: $n = 6$, 171.06% ± 11.98%; $p > 0.05$). The obtained results support the hypothesis that the activation of the IL-17RA transduction pathway can influence hippocampal synaptic plasticity, with a specific role played by p38 MAPK.

Altered synaptic plasticity is paralleled by increased IL-17A levels during experimental autoimmune encephalomyelitis (EAE)

In order to investigate the possible upregulation of the IL-17 axis in an experimental model of MS, we performed a parallel analysis of synaptic plasticity and hippocampal IL-17A levels at two different time points of chronic-relapsing experimental autoimmune encephalomyelitis (crEAE) by using electrophysiological recordings and an independent ELISA assay. The levels of hippocampal IL-17A were found to be significantly higher than those under control conditions during the acute clinical phase of crEAE (acute crEAE, days 15–18 post-inoculation

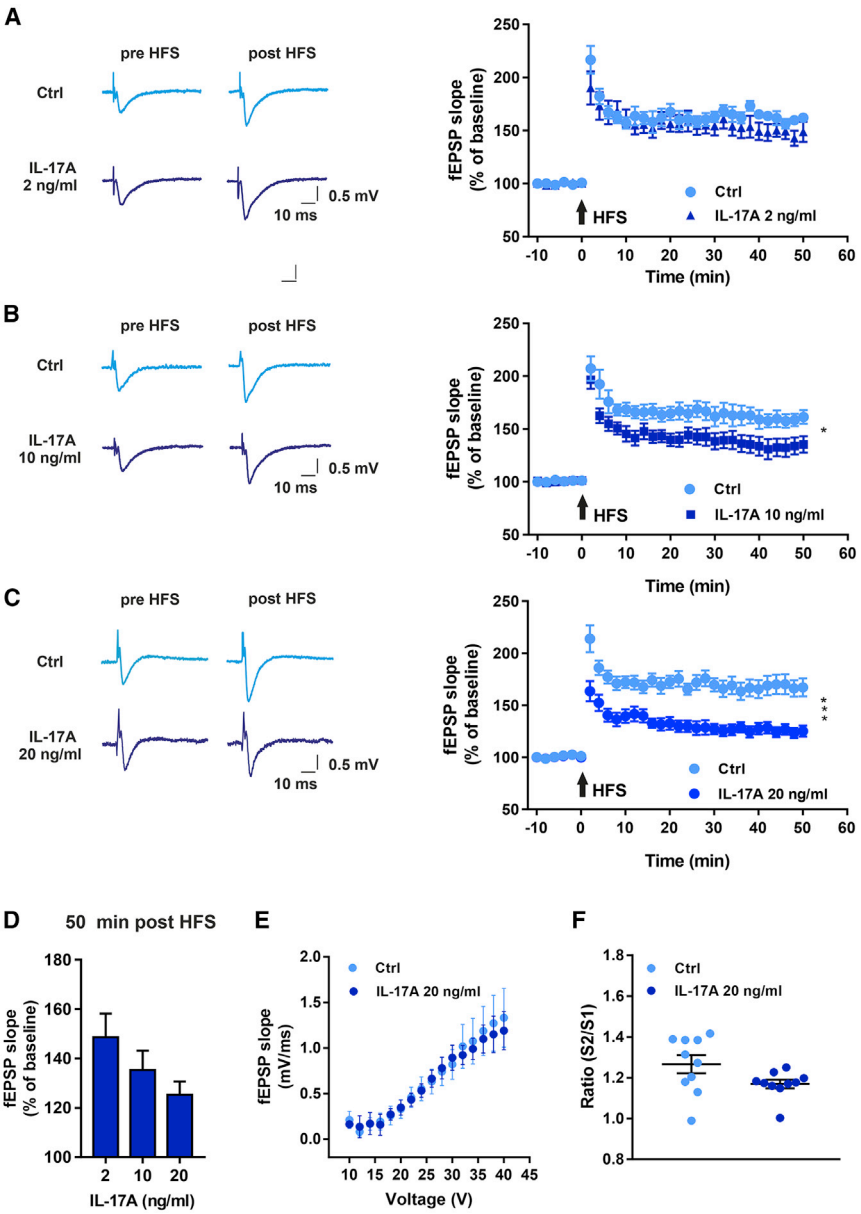

Figure 1. Hippocampal LTP is dose-dependently blocked by exposure to IL-17A

(A–C) Graphs showing the time-course of the fEPSP slope recorded from the hippocampal CA1 area under control conditions (Ctrl, light-blue-filled circles) and after exposure to increasing doses of IL-17A. (A) Ctrl: n = 7, 162.11% ± 3.66%; IL-17A, 2 ng/mL (blue-filled triangles): n = 10, 148.66% ± 9.55%. (B) Ctrl: n = 8, 161.45% ± 6.59%; IL-17A, 10 ng/mL (blue-filled squares): n = 9, 135.38% ± 7.79%. (C) Ctrl: n = 8, 167.22% ± 8.72%; IL-17A, 20 ng/mL (blue-filled circles): n = 13, 125.32% ± 5.38%. Example fEPSP traces on the left were acquired before and after the HFS protocol. Note the disruption of hippocampal LTP induction in slices exposed to IL-17A 10 ng/mL (B) and 20 ng/mL (C).

(D) Graph showing the dose-dependent relationship occurring between IL-17A concentrations and the fEPSP slope recorded 50 min after HFS.

(E and F) Graph showing the input-output curve (E) and 50-ms paired-pulse facilitation (F) recorded from the hippocampal CA1 area under control conditions (Ctrl, light-blue-filled circles) and after exposure to 20 ng/mL IL-17A (blue-filled circles). (E) Ctrl: n = 5; IL-17A, 20 ng/mL: n = 7. (F) Ctrl: n = 10, ratio S2/S1 of 1.26 ± 0.04; IL-17A, 20 ng/mL: n = 10, ratio S2/S1 of 1.16 ± 0.02. HFS, high-frequency stimulation. Data are presented as the mean ± SEM (*p < 0.05; ***p < 0.001).

[p.i.]) ($p < 0.05$; Figure 3A). At the same time point, hippocampal plasticity, as previously demonstrated (Di Filippo et al., 2013), was found to be altered with respect to control conditions ($p < 0.001$; Figure 3B). The alteration of hippocampal LTP was confirmed by also applying the TBS induction protocol for LTP during the acute phase of EAE ($p < 0.001$; Figure S1A). Conversely, later in the disease course (recovery crEAE, >30 days p.i.), hippocampal IL-17A levels were characterized by a decrement toward control levels ($p > 0.05$; Figure 3A), and plasticity at the same time point was found to be normally expressed (recovery crEAE versus Ctrl: $p > 0.05$; recovery crEAE versus acute crEAE: $p < 0.05$; Figure 3B). Collectively, these results demonstrate the co-occurrence of hippocampal LTP impairment and IL-17A overexpression in the hippocampus of crEAE mice during the acute inflammatory phase, with a subsequent recovery paralleled by a reduction in IL-17A levels.

Acute *in vitro* blockade of IL-17A ameliorates synaptic deficits during EAE

In order to confirm the potential involvement of the IL-17A pathway in EAE-related synaptopathy, we investigated if the *in vitro* exposure to antibodies (Ab) blocking the cytokine was able to influence the impairment of LTP. To this aim, we exposed brain slices obtained from acute crEAE mice to 1 μg/mL anti-IL-17A Ab for 1 h and then performed electrophysiological recordings, showing a partial recovery of LTP ($0.001 < p < 0.01$; Bonferroni Post hoc test: $p < 0.001$ during the early LTP phase; Figure 3C). This evidence suggests that even a short-term blockade of the IL-17 axis prior to the high frequency stimulation (HFS) protocol is able to partially counteract plasticity loss during neuroinflammation, further identifying this molecule and its downstream pathway as potential targets for therapeutic approaches aimed at preserving plasticity during MS. Exposure of brain slices to control immunoglobulin G (IgG) (1 μg/mL for 1 h) did not influence hippocampal LTP during pathological neuroinflammation (EAE, n = 7, 126.61% ± 7.42%; EAE plus control IgG, n = 6, 127.82% ± 9.88%; $p > 0.05$).

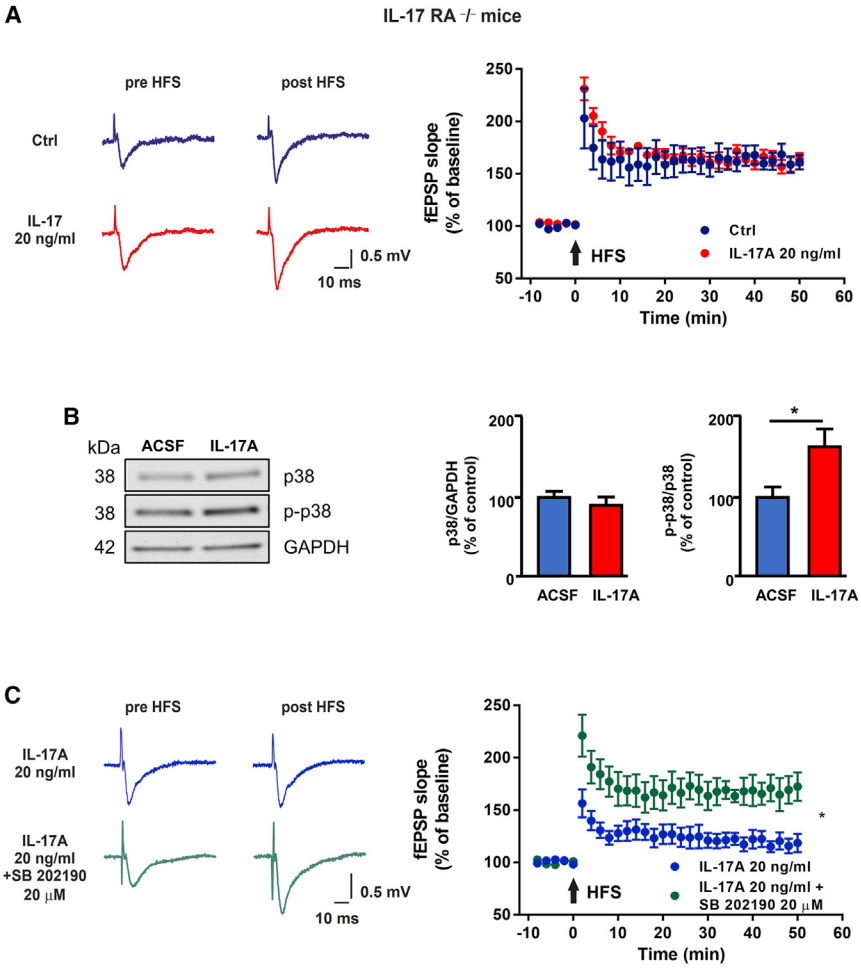

Figure 2. The synaptic effects of IL-17A are mediated by IL-17RA and p38 MAPK activation

(A) Graph showing the time-course of the fEPSP slope recorded from the hippocampal CA1 area in IL-17RA$^{-/-}$. Exposure to 20 ng/mL IL-17A does not modify synaptic potentiation (LTP) in IL-17RA$^{-/-}$ mice (IL-17RA$^{-/-}$ [blue-filled circle]: n = 5, 160.99% ± 6.80%; IL-17RA$^{-/-}$ plus IL-17A 20 ng/mL [red-filled circles]: n = 8, 163.98% ± 5.79%). Example fEPSP traces on the left were acquired before and after the HFS protocol.

(B) Western blot analysis of total (p38) and phosphorylated p38 (p-p38) in hippocampal slices exposed for 1 h to 20 ng/mL IL-17A (on the left) and densitometric quantification of changes in gray values (on the right) (p38/GAPDH: ACSF [blue]: n = 7, 100 ± 3.89; IL-17A 20 ng/mL [red]: n = 7, 97.43 ± 8.39; p-p38/p38: ACSF [blue]: n = 7, 99.71 ± 11.02; IL-17A 20 ng/mL [red]: n = 7, 164.3 ± 24.68).

(C) The co-exposure to a p38 MAPK inhibitor, 20 μM SB 202190, and 20 ng/mL IL-17 is able to rescue the LTP disruption induced by 20 ng/mL IL-17A alone in control mice (IL-17A 20 ng/mL [blue-filled circles]: n = 7, 118.56% ± 8.72%; IL-17A 20 ng/mL plus 20 μM SB 202190 [green-filled circles]: n = 6, 172.42% ± 13.49%). Example fEPSP traces on the left were acquired before and after the HFS protocol. Data are presented as the mean ± SEM (*p < 0.05).

Behavioral tests demonstrate preserved learning processes in EAE mice lacking IL-17A

It has been already shown that the pathogenic process characterizing EAE is able to induce cognitive/behavioral deficits at different time points during the course of the disease (Di Filippo et al., 2018), even before the development of clinical motor deficits (Dutra et al., 2013). In order to investigate the contribution of IL-17A on EAE-related CI, we induced the experimental disease in mice lacking IL-17A (IL-17A$^{-/-}$) and assessed their memory performance through an open-field hole-board test, which has been used to assess hippocampal-based cognitive tasks (Di Filippo et al., 2016; Lemon and Manahan-Vaughan, 2006). In this test, the reduction of the total number of head-dipping into holes (hole exploration) between the first and the second session is considered an expression of learning and recognition (Di Filippo et al., 2016; Lemon and Manahan-Vaughan, 2006). We analyzed the performance of four different experimental groups, as follows: control wild-type mice (Ctrl), mice lacking IL-17A (IL-17A$^{-/-}$), wild-type mice affected by EAE (EAE), and mice lacking IL-17A affected by EAE (EAE IL-17A$^{-/-}$). In order to avoid potential confounding factors due to EAE-related motor deficits, we performed the test in the early pre-motor phase of the experimental disease (10–12 days p.i.), when the neurological disability score of involved mice was equal to 0. In this early disease phase, hippocampal LTP induction was found to be already impaired despite the absence of clinically detectable motor deficits (0.001 < p < 0.01; Figure S1D). It should be noted that other studies reported that mice lacking IL-17A are partially resistant to EAE induction (Komiyama et al., 2006; McGinley et al., 2020), whereas others suggested a minor role in the course of experimental disease (Haak et al., 2008). Interestingly, in mice of the EAE group (n = 10), we found a slightly earlier onset of the disease motor signs with respect to the EAE IL-17A$^{-/-}$ group (n = 10) (EAE: disease onset at 15.89 ± 0.45 days p.i.; EAE IL-17A$^{-/-}$: disease onset at 16.37 ± 0.26 days p.i.). However, the mean neurological disability score at disease peak was not significantly different between the two groups (EAE: n = 10, 1.15 ± 0.46; EAE IL-17A$^{-/-}$: n = 10, 1.00 ± 0.24; p > 0.05). Differences in the induction protocols and experimental conditions might account for the reported various outcomes of EAE induction in mice lacking IL-17A. A behavioral analysis showed that both Ctrl and IL-17A$^{-/-}$ mice without the experimental disease were characterized by a significantly reduced number of hole explorations when re-exposed to the hole-board compared with their initial performance (session II versus session I, p < 0.001; Figure 4A), suggesting the occurrence of learning processes. Conversely, in wild-type mice affected by EAE, there was no significant difference in the number of hole explorations after hole-board re-exposure (session II versus session I, p > 0.05; Figure 4A), confirming the presence of context recognition deficits in this model.

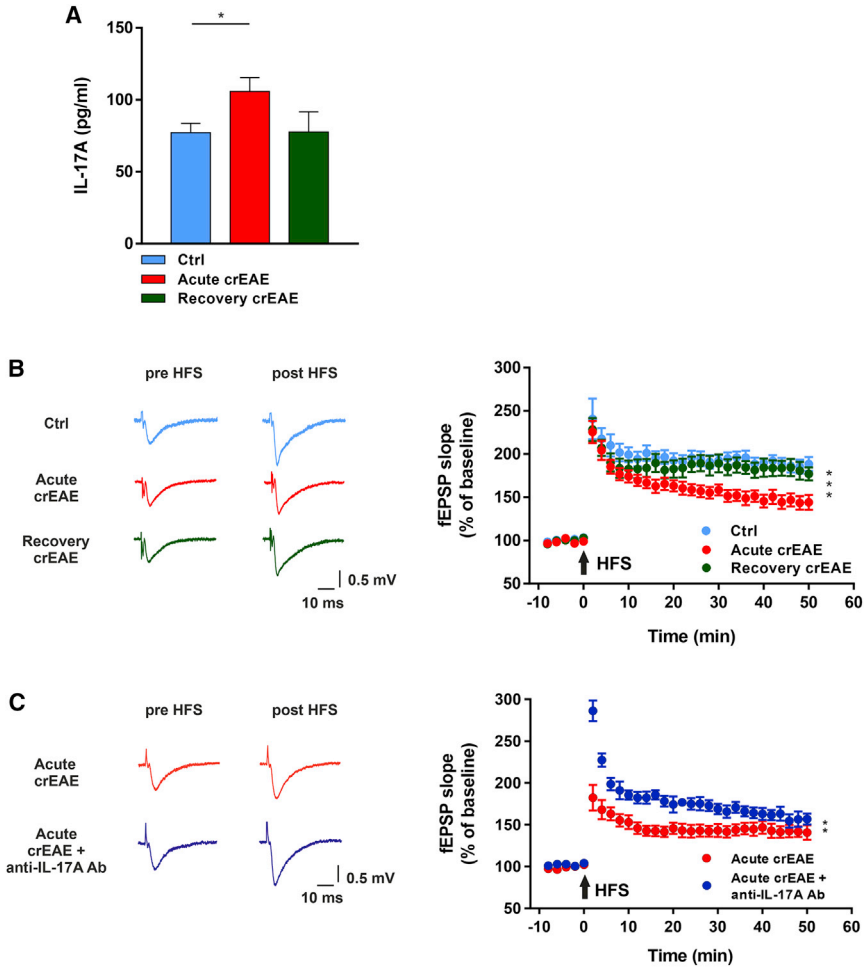

Figure 3. Synaptic plasticity deficits and expression levels of IL-17A in the hippocampus

(A) Graph showing ELISA assays of hippocampal IL-17A levels under control conditions, during acute crEAE and recovery crEAE (Ctrl [light blue]: n = 7, 77.14 ± 6.48 pg/mL; acute crEAE [red]: n = 10, 105.8 ± 9.68 pg/mL; recovery crEAE [green]: n = 6, 77.67 ± 14.07 pg/mL).

(B) Graph showing the time-course of the fEPSP slope recorded from the hippocampal CA1 area under control conditions, in mice affected by the acute relapsing phase of crEAE and by the late recovery phase of crEAE (Ctrl [light-blue-filled circles]: n = 13, 188.52% ± 8.13%; acute crEAE [red-filled circles]: n = 15, 144.20% ± 8.66%; recovery crEAE [green-filled circles]: n = 11, 177.06% ± 7.51%; acute crEAE versus Ctrl: $p < 0.001$). Example fEPSP traces on the left were acquired before and after the HFS protocol.

(C) Graph showing the time-course of the fEPSP slope recorded in the hippocampal CA1 area of acute crEAE group under control conditions and after exposure to 1 μg/mL anti-IL-17A Ab (acute crEAE [red-filled circles]: n = 12, 140.66% ± 8.75%; acute crEAE plus anti-IL-17A Ab [blue-filled circles]: n = 10, 156.84% ± 6.47%). Example fEPSP traces on the left were acquired before and after the HFS protocol. Data are presented as the mean ± SEM (*$p < 0.05$; **$0.001 < p < 0.01$; ***$p < 0.001$).

The impaired performance was reversed when EAE was induced in IL-17A$^{-/-}$ mice, which indeed showed a significantly reduced number of hole exploration in the second session compared to that of the first one (session II versus session I, $p < 0.001$; Figure 4A). Accordingly, the percent reduction of hole explorations between the second and the first hole-board sessions showed a statistically significant difference between the EAE group and the other groups (EAE versus EAE IL-17A$^{-/-}$: $0.001 < p < 0.01$; EAE versus Ctrl: $p < 0.05$; EAE versus IL-17A$^{-/-}$: $p < 0.05$; Figure 4B). All of these results suggest that the absence of IL-17A is associated with preserved learning processes during EAE. The analysis of the mean motor performance during the hole-board test, expressed as the number of crossings among four equal-sized squares in which the arena was divided, revealed no significant difference between the two groups with the experimental disease (EAE versus EAE IL-17A$^{-/-}$, $p > 0.05$) (Figure 4C). It should be noted that, even in the absence of clinically evident motor deficits, both of the groups affected by EAE displayed a reduced horizontal activity with respect to healthy mice (Ctrl versus EAE: $0.001 < p < 0.01$; IL-17A$^{-/-}$ versus EAE IL-17A$^{-/-}$: $0.001 < p < 0.01$; Figure 4C). This observation could rely on the presence of an inflammation-related behavior with altered basal exploration occurring during the experimental disease.

Expression patterns of IL-17A and IL-17RA in different cell types suggest a direct neuro-immune interaction in the hippocampus

In order to characterize the cellular cross-talk underlying the synaptic effects of IL-17A, we investigated the specific localization of the cytokine and its receptor in the hippocampal CA1 region as well as their phenotypic expression through triple or double immunofluorescence for IL-17A or IL-17RA with NeuN, a neuronal marker; glial fibrillary acidic protein (GFAP), an astrocyte marker; and Iba-1, a microglia marker. The results showed that, both in control (Ctrl) and acute crEAE mice, Il-17A co-localizes with Iba-1-positive microglia (Figures 5A and 5B) but not with the neuronal marker NeuN (Figures 5C and 5D) and the astrocyte marker GFAP (Figures 5E and 5F), as confirmed by co-localization analyses (Table 1). This result is in line with existing literature that showed that microglial cells can produce IL-17A after being exposed to interleukin-23 (IL-23) or interleukin-1β (IL-1β) (Kawanokuchi et al., 2008). Conversely, IL-17RA was primarily expressed on CA1 neurons (Figures 6A and 6B) and in fine processes of some GFAP-positive astrocytes (Figures 6A and 6B) but not in Iba-1-positive microglia (Figures 6C and 6D), as confirmed by co-localization analyses (Table 1). Of note, the specificity of the anti-IL17RA staining was confirmed

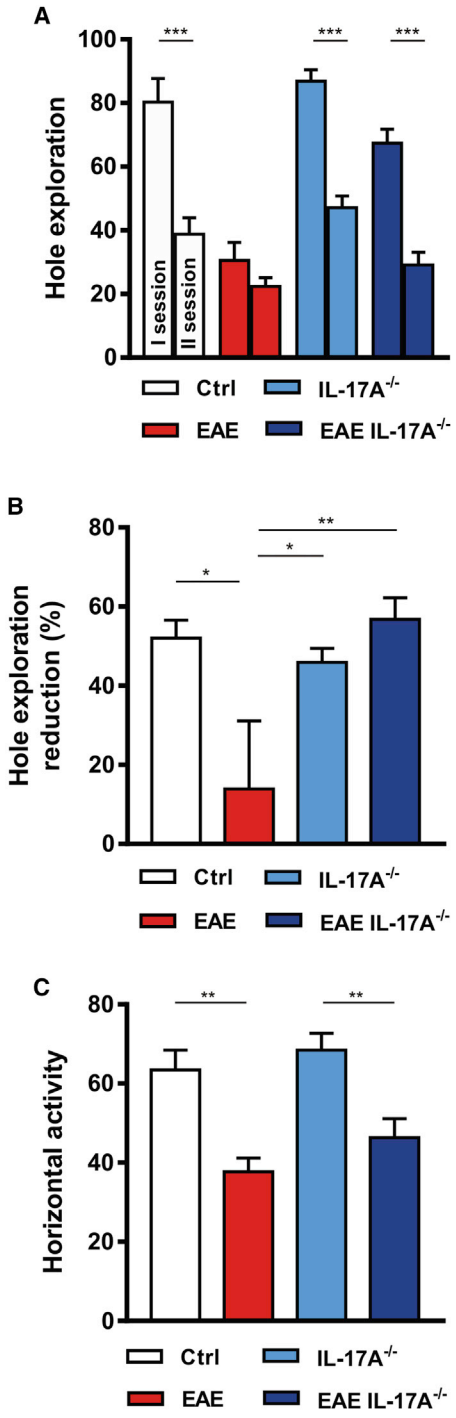

Figure 4. The performance in the hole-board learning test is preserved in EAE mice lacking IL-17A

(A) Histograms showing the hole exploration activity as the number of head-dippings during a 2-session hole-board test in control wild-type mice (white), wild-type mice affected by EAE (red), IL-17A$^{-/-}$ mice (light blue), and IL-17A$^{-/-}$ mice affected by EAE (blue) (Ctrl: n = 10; I session: 80.3 ± 7.36; II session: 38.8 ± 5.18; EAE: n = 8; I session: 30.50 ± 5.69; II session: 22.25 ± 2.71; IL-17A$^{-/-}$: n = 11; I session: 86.91 ± 3.54; II session: 47.09 ± 3.65; EAE IL-17A$^{-/-}$: n = 10; I session: 67.40 ± 4.38; II session: 29.10 ± 4.05).

(B) Graph showing the percent reduction of total head-dippings between the first and the second session during the hole-board test in all the four experimental groups (Ctrl [white]: n = 10, 52.06% ± 4.53%; EAE [red]: n = 8, 13.89% ± 17.21%; IL-17A$^{-/-}$ [light blue]: n = 11, 45.89% ± 3.51%; EAE IL-17A$^{-/-}$ [blue]: n = 10, 56.79% ± 5.42%).

(C) Graph showing the mean horizontal locomotor activity of the four experimental groups during the test (Ctrl [white]: n = 10, 63.4 ± 5.04; EAE [red]: n = 8, 37.69 ± 3.45; IL-17A$^{-/-}$ [light blue]: n = 11, 68.45 ± 4.25; EAE IL-17A$^{-/-}$ [blue]: n = 10, 46.30 ± 4.76). Data are presented as the mean ± SEM (*$p < 0.05$; **$0.001 < p < 0.01$; ***$p < 0.001$).

by performing immunofluorescence in mice lacking IL-17RA (Figure S2A). This differential localization of IL-17A and IL-17RA in CA1 hippocampal cell types seems to suggest that IL17 primarily produced by microglial cells could directly act on IL-17RA neuronal receptors, supporting a key role of this molecule in the hippocampal neuro-immune cross-talk. Moreover, we assessed the p-p38 MAPK expression level in CA1 of both control and acute crEAE mice. In line with the hypothesis of an IL-17RA-dependent activation of p38 MAPK in hippocampal neurons during neuroinflammation, we observed that the p-p38 MAPK expression level in CA1 of control mice was almost absent, whereas it was higher in crEAE mice (Figure S2B). Furthermore, a confocal analysis demonstrated that p-p38 MAPK was expressed in CA1 hippocampal neurons during crEAE (Figure S2B). Lastly, a densitometric analysis of the IL-17A and IL-17RA expression level in CA1 showed that acute crEAE mice were characterized by higher IL-17A expression levels than controls in the hippocampus ($p < 0.0001$; Figure 5G) and other brain areas such as the motor cortex and the thalamus ($p < 0.0001$). No differences were observed with regard to IL-17RA expression between crEAE and Ctrl mice ($p > 0.05$; Figure 5H). This latter result suggests an important role of activated microglia as a cellular source of the increased IL-17A levels in the hippocampal CA1 area during the acute phase of the experimental disease.

DISCUSSION

For a long time, the CNS was considered an immune-privileged "sanctuary," with a subsequent underestimation of the influence exerted by immune cells on neuronal and synaptic function. During the last decades, it has been established that the immune system and neural networks are characterized by a continual cross-talk with a significant effect on human cognition and behavior, both during physiological and pathological conditions (Dantzer et al., 2008; Di Filippo et al., 2008). The secretion of immune mediators during neuro-inflammatory processes has the potential to influence synaptic/neuronal function, contributing to disabling symptoms of MS, such as CI (Di Filippo et al., 2018). In this scenario, synaptic LTP represents an interesting plastic phenomenon to be analyzed because it displays all of the expected hallmarks for a biological learning process (Nicoll, 2017) and participates in the formation of synaptic connectivity maps and memory engrams (Asok et al., 2019) in parallel with cell-autonomous changes in membrane excitability (Titley et al., 2017).

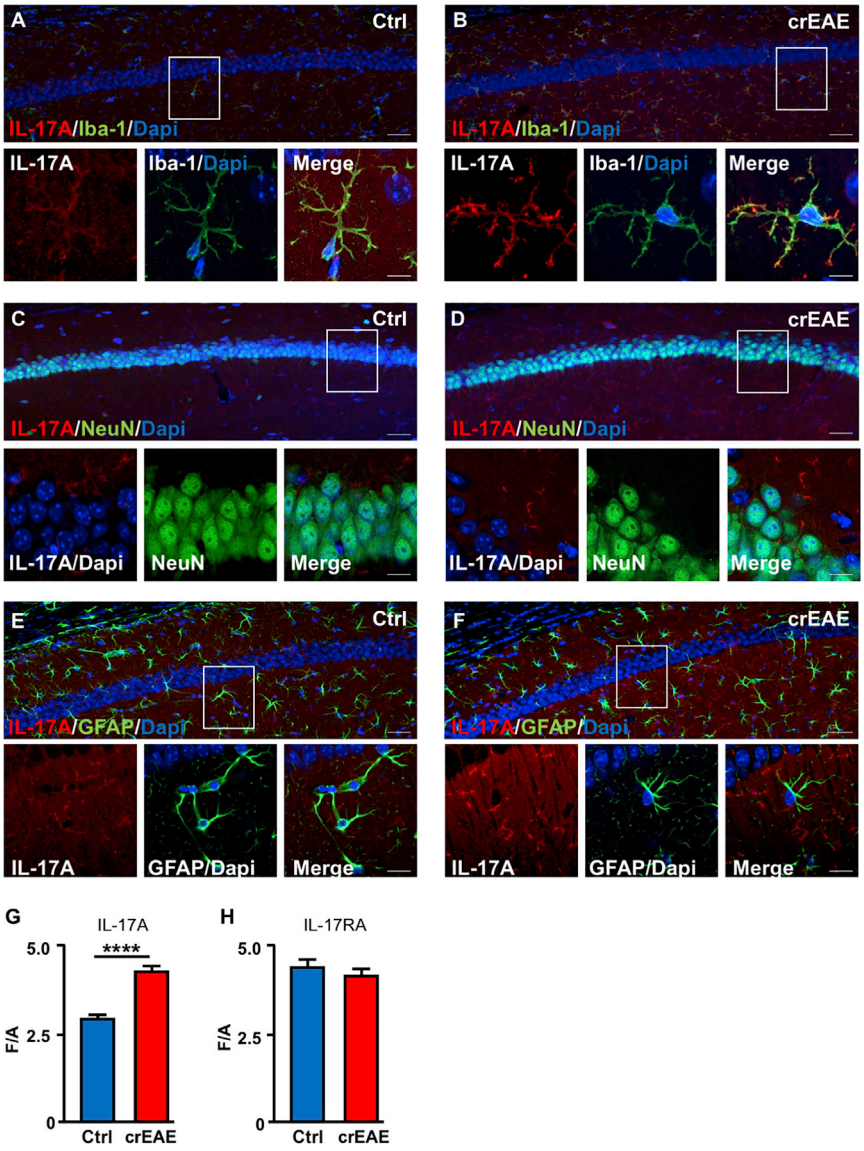

Figure 5. Hippocampal expression of IL-17A under control conditions and during the acute phase of crEAE

(A and B) Immunofluorescence double labeling of IL-17A (red) with microglia marker Iba-1 (green) and 4′,6-diamidino-2-phenylindole (DAPI) counterstaining (blue) in the CA1 hippocampal region of control (Ctrl) and acute crEAE mice showing the IL-17A co-localization with Iba-1-positive microglia. Each box of (A) and (B) shows images that represent the area of interest for the higher magnification of the three underlying images (single and merged images).

(C and D) Immunofluorescence double labeling of IL-17A (red) with the neuronal marker NeuN (green) and DAPI counterstaining (blue) in the CA1 hippocampal region of Ctrl and acute crEAE mice showing the lack of co-localization between IL-17A and NeuN. Each box of (C) and (D) images represents the area of interest for the higher magnification of the three underlying images (single and merged images).

(E and F) Immunofluorescence double labeling of IL-17A (red) with the astrocyte marker GFAP (green) and DAPI counterstaining (blue) in the CA1 hippocampal region of Ctrl and crEAE mice showing the lack of co-localization between IL-17A and GFAP. Each box of (E) and (F) images represents the area of interest for the higher magnification of the three underlying images (single and merged images). The scale bars represent 50 μm (A, B, C, D, E, and F), 20 μm (boxes of C, D, E, and F), and 15 μm (boxes of A and B).

(G and H) Histograms of the densitometric analysis of IL-17A (G) and IL-17RA (H) immunoreactivity in the CA1 of Ctrl and acute crEAE mice. The F/A ratio defines the mean fluorescence of individual samples (F) normalized to total surface (A). Ctrl and crEAE: n = 5 animals (10 samples/animal). Data are presented as the mean ± SEM (****$p < 0.0001$).

In this work, we show that hippocampal synaptic plasticity is dose-dependently disrupted by IL-17A. The immunopathogenic view of MS has significantly changed during the last decades, turning from the Th1/Th2-centered classical paradigm to a more complex scenario involving IL-17-producing Th cells (Rostami and Ciric, 2013; Waisman et al., 2015). The molecular mechanisms underlying IL-17A effects are still under investigation, and interestingly, this cytokine could be involved in a wider and more complex neuro-immune interaction. Indeed, it has been demonstrated that IL-17A can act directly on neurons to alter their sensory response, modulating the behavior of *Caenorhabditis elegans* (Chen et al., 2017). Moreover, IL-17A can negatively modulate hippocampal neurogenesis, and the lack of this cytokine is associated with enhanced intrinsic neuronal excitability and basal excitatory synaptic transmission in the hippocampal dentate gyrus (DG) (Liu et al., 2014). This evidence supports a role for IL-17A in shaping neuronal development and functions, which goes beyond its immunological activities. Interestingly, recent work showed that a subset of meningeal-resident γδ T cells exerts a physiological role in cognition, through the secretion of IL-17A (Ribeiro et al., 2019). Specifically, the absence of IL-17A was not associated with abnormal hippocampal synaptic plasticity under control conditions, but the cytokine was found to be required to express hippocampal LTP after a short-term memory task (Ribeiro et al., 2019). All of these observations, together with our results, suggest that IL-17A may act as a bi-modal synaptic modulator, similarly to other soluble immune mediators, such as IL-1β (Di Filippo et al., 2008, 2016; Schneider et al., 1998). IL-17A is required at low concentrations for physiological synaptic function and becomes detrimental to synapses and cognition when overexpressed following inflammatory stimuli or pathological conditions such as MS.

We found several elements suggesting a link between IL-17A and hippocampal dysfunction during neuroinflammatory processes. The acute relapsing phase of crEAE was indeed characterized by a significant increase in IL-17A expression,

Table 1. Markers of co-localization in hippocampal CA1 region of control (Ctrl) and EAE mice

Markers of co-localization	CCP of: Ctrl	crEAE
IL-17A/GFAP	0.0184	0
IL-17A/Iba-1	0.1617	0.4601
IL-17A/NeuN	0	0
IL-17RA/GFAP	0.0433	0.2357
IL-17RA/Iba-1	0.0284	0.0264
IL-17RA/NeuN	0.4307	0.3944

To examine the degree of co-localization between IL-17A or IL-17RA and Iba-1, NeuN, and GFAP in the hippocampal CA1 region of Ctrl and crEAE mice, the correlation coefficient of Pearson (CCP) was used (Zeiss LSM800 software). The coefficient range is 0 to ± 1 with 0 corresponding to non-overlapping and 1 reflecting 100% co-localization. Higher CCP values correspond to a strong co-localization.

paralleled by a disruption of hippocampal LTP, that was lately recovered together with a reduction of the cytokine levels in the hippocampus. These results suggest that the dynamic changes of synaptic function that characterize EAE occur in a strict temporal relationship with fluctuations in IL-17A expression levels. In line with this evidence, the *in vitro* short-term treatment with anti-IL-17A Ab was found to ameliorate hippocampal synaptic plasticity alterations. Notably, the beneficial effects of IL17 axis blockade on LTP expression were, although statistically significant, only partial and more evident in the early LTP phase. This could be due to at least two main reasons. First, IL-17A might not be the only soluble immune molecule exerting a negative effect on synaptic function, but more likely, it could act in concert with other cytokines and/or oxygen radicals (Di Filippo et al., 2018). Second, an *in vitro* short-term inhibition (1 h) of the IL-17 axis with Ab may not be sufficient to reverse all the downstream cellular effects already triggered by the prolonged exposure of the brain tissue to pathological concentrations of the cytokine.

IL-17A induces its effects via the IL-17R family of receptors (which are composed of homo- or heterodimeric subunits), most commonly through IL-17RA (Ely et al., 2009). The negative effects exerted by IL-17A on LTP induction were found to be mediated by the specific activation of its receptor and, among the downstream pathways activated by IL-17RA, by the kinase p38 MAPK. The exposure of brain slices to IL-17A was indeed found to result in the phosphorylation of the kinase, and the pharmacological blockade of p38 MAPK was able to reverse the synaptic deficits induced by the cytokine. The activation of IL-17RA leads to an amplification of the inflammatory process. Among the different actors involved in this transduction pathway, p38 MAPK and nuclear factor kappa B (NF-κB) seem to play a crucial role (Xu and Cao, 2010; Zepp et al., 2011). The MAPK family members are indeed implicated in regulating a range of biological responses from cell proliferation, survival, differentiation, and migration to inflammation and cancer, in a cell-context-specific and cell-type-specific manner (Wagner and Nebreda, 2009). Specifically, p38 MAPK is able to mediate the expression of pro-inflammatory factors, like cyclooxygenase 2 (COX2), and many other pro-inflammatory cytokines, such as tumor necrosis factor-α (TNF-α), IL-1β, and interleukin-6 (IL-6).

Because we found that IL-17RA is also expressed in fine processes of some hippocampal astrocytes, one should consider the possibility that IL-17A could induce the release by glial cells of other mediators with a detrimental synaptic effect. However, accumulating evidence (Chen et al., 2017; Reed et al., 2020; Ribeiro et al., 2019) suggests that IL-17A might directly act on the neuronal receptor to exert its functions as a neuromodulator. It has been shown that IL17R is expressed by hippocampal neurons (Wang et al., 2009) and mice in which IL-17RA was conditionally deleted on astrocytes and microglia did not recapitulate the short-term memory abnormalities seen in mice lacking IL-17A in all cell types (Ribeiro et al., 2019), suggesting an effect of IL-17A on the neuronal cellular populations. Similarly, it has been suggested that IL-17A is able to influence the behavior of a mouse model of neurodevelopmental disorder, acting through a direct modulation of IL-17R-expressing neurons in the primary somatosensory cortex (Reed et al., 2020). In line with this evidence, our quantitative analysis of histochemical data showed that in the CA1 hippocampal area the IL-17RA is primarily expressed on hippocampal CA1 neurons and that increased levels of p-p38 MAPK can be found in hippocampal neurons during the acute phase of crEAE, strengthening the link among IL-17A overexpression, neuronal IL-17RA activation, and hippocampal synaptic plasticity disruption during neuroinflammatory disorders.

Interestingly, our results also show that the cellular source of IL-17A in the CA1 hippocampal area is primarily represented by microglial cells, pointing toward a role of this cytokine in the communication between different cellular populations in the hippocampal microenvironment not only during EAE but also under physiological conditions. It has been proposed that the production of IL-17A by microglial cells may be triggered by the exposure to other pro-inflammatory cytokines, such as IL-23 and IL-1β, or by the activation of the Toll-like receptor 2 (TLR-2) during CNS-damaging insults (Kawanokuchi et al., 2008; Lv et al., 2011). The study of conditional transgenic murine models lacking IL-17RA in specific cellular populations could represent a promising future line of research to better define the mechanisms and consequences of IL-17A production by glial cells.

Because synaptic plasticity represents the putative basis for cognitive and memory processes, its disruption could result in cognitive alterations. Indeed, spatial novelty recognition during the hole-board test was found to rely on hippocampal synaptic plastic changes (Lemon and Manahan-Vaughan, 2006), and the EAE-dependent hippocampal synaptic dysfunction is coupled with cognitive and behavioral alterations (Di Filippo et al., 2018). In this work, we confirm that an impairment in behavioral/cognitive abilities can be detected even before the onset of the classical motor manifestations of the experimental disease, in parallel with altered synaptic plasticity in the hippocampus, and that it is reversed in the absence of IL-17A in KO mice. In our experimental setting, in order to prevent a confounding effect of motor impairment on behavioral tests, control EAE mice and EAE IL-17A KO mice were tested at the

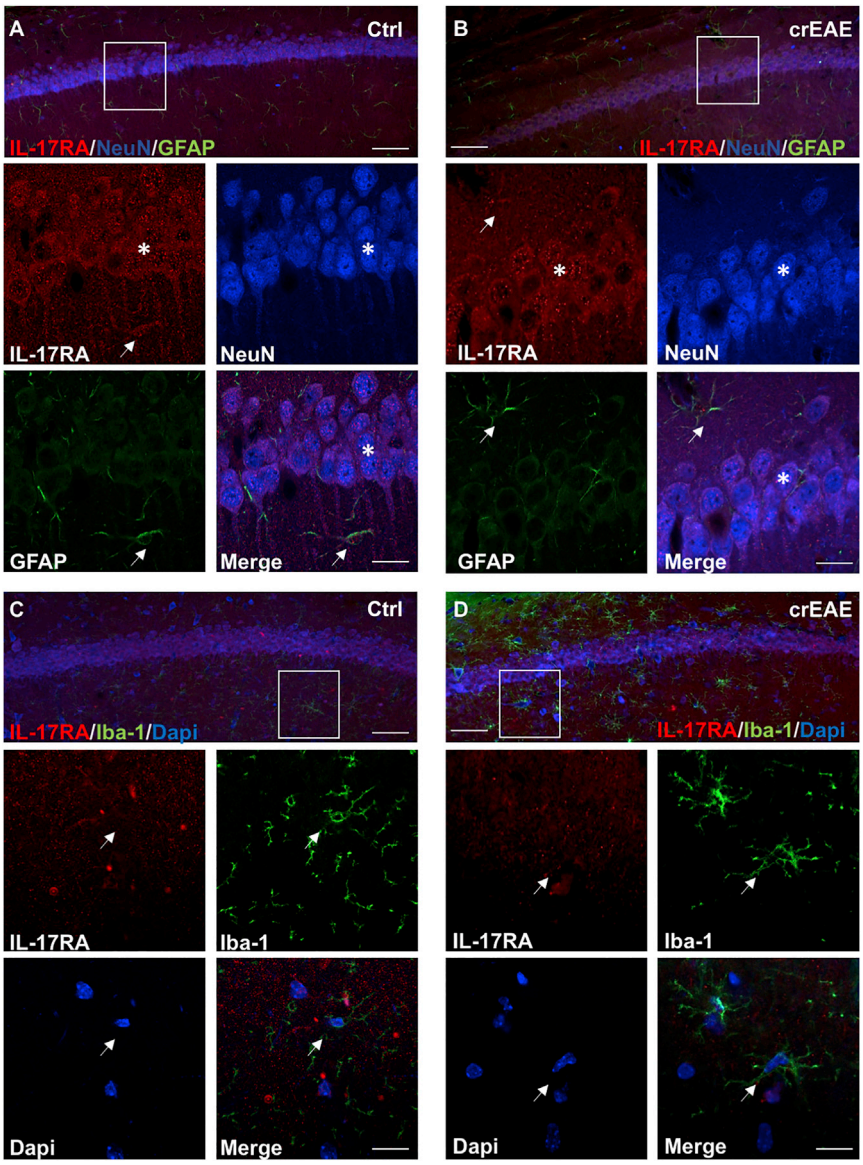

Figure 6. Hippocampal expression of IL-17RA under control conditions and during the acute relapsing phase of crEAE

(A and B) Immunofluorescence triple labeling of IL-17RA (red) with neuronal marker NeuN (blue) and astrocyte marker GFAP (green) in the CA1 hippocampal region of Ctrl and acute crEAE mice showing the IL-17RA co-localization with NeuN (asterisks) and with some fine processes of GFAP-positive astrocytes (arrows).

(C and D) Immunofluorescence double labeling of IL-17RA (red) with microglia marker Iba-1 (green) and DAPI counterstaining (blue) in the CA1 hippocampal region of Ctrl and acute crEAE mice showing the lack of co-localization between IL-17RA and Iba-1 (arrows). Each box of the top images is enlarged into four separate pictures (below) with single and merged images. The scale bars represent 50 μm (A, B, C, and D) and 20 μm (enlarged boxes of A, B, C, and D). Ctrl and crEAE: n = 5 animals (10 samples/animal).

same time point, before the onset of motor symptoms of the disease, with a clinical score equal to 0. It has been shown that when neurological disability is scored below 1.5, EAE animals usually retain maximum motor performance assessed with Rotarod (van den Berg et al., 2016), thus limiting the influence of motor disability on behavioral tests. Of note, the presence of a hippocampal-dependent visuo-spatial learning impairment during the course of EAE is supported by previous work (Di Filippo et al., 2016; Kim et al., 2012), but the overall cognitive performance might have been influenced by the presence of early EAE-related anxiety (Haji et al., 2012) and/or deficits in other cognitive domains (Olechowski et al., 2013). Overall, our results suggest that preventing the over-activation of the IL-17 axis might counteract the hippocampal-dependent cognitive deficits associated with the disease, and a thorough evaluation of how IL-17A may differently modulate brain networks subserving other cognitive domains and/or mood and behavior during neuroinflammatory processes could represent a future interesting field of research.

Interestingly, it has been shown that serum levels of IL-17A are significantly higher in individuals with MS-related CI (Trenova et al., 2018), supporting the hypothesis of the involvement of this cytokine in the cognitive performance of human subjects, a possibility that needs further investigations. Taken together, the results of the present study confirm the emerging key role of IL-17A in the neuro-immune cross-talk occurring in the hippocampal CA1 area. Also, they demonstrate that this cytokine has the potential to exert detrimental effects on synaptic plasticity in the hippocampal circuit, suggesting new potential targets for therapeutic strategies aimed at counteracting inflammatory synaptopathy and impaired cognition during MS.

LIMITATIONS OF THE STUDY

The behavioral experiments that we performed suggest that the induction of EAE in mice lacking IL-17A is associated with preserved cognitive abilities during the course of EAE, potentially due to the lack of the detrimental effect that the overexpression of this cytokine exerts on hippocampal synaptic plasticity. However, it should be noted that the absence of IL-17A might also result in a milder EAE course, which could per se explain preserved cognitive functions in this experimental group. Our experimental design indeed does not exclude the possibility that a more intense brain and systemic inflammatory reaction was present in wild-type EAE mice because this latter

experimental group developed a slightly anticipated acute phase of the disease with respect to EAE induced in IL-17A KO mice. Moreover, the alteration of the IL-17 axis might alter gut flora (Fleming et al., 2017), potentially acting as an additional confounding factor for behavioral tests (Cryan and Dinan, 2012). The specific neuro-modulatory role played by IL-17A in the CNS might be thus confirmed by future studies investigating the cognitive and behavioral effects of *in vivo* treatments with anti-IL-17A Ab or anti-p38 MAPK strategies, during the acute relapsing phase of EAE, avoiding the potential confounding factor represented by systemic immune modulation linked to the genetic manipulation of the IL-17 axis. At the same time, as previously discussed, the investigation of transgenic models selectively lacking IL-17RA in specific cell lines might help in understanding if the synaptic effects of IL-17A are directly triggered by the neuronal IL-17RA or rather induced by other immune mediators released by glial cells, with known neuromodulatory effects. To date, different immune cell types and soluble mediators have been identified as potential actors in MS-related synaptopathy. Future studies should help to untangle the specific neuro-immune role played by the IL-17 axis in this complex scenario.

STAR★METHODS

Detailed methods are provided in the online version of this paper and include the following:

- KEY RESOURCES TABLE
- RESOURCE AVAILABILITY
  - Lead contact
  - Materials availability
  - Data and code availability
- EXPERIMENTAL MODEL AND SUBJECT DETAILS
  - Animals and induction of experimental autoimmune encephalomyelitis
- METHOD DETAILS
  - Electrophysiology
  - Measurement of hippocampal IL-17A levels
  - Immunofluorescence
  - Western blot
  - Hole-board behavioral test
  - Drugs
- QUANTIFICATION AND STATISTICAL ANALYSIS
  - Clinical scoring of experimental autoimmune encephalomyelitis
  - Electrophysiology
  - Measurement of hippocampal IL-17A levels
  - Immunofluorescence
  - Western blot
  - Hole-board behavioral test

SUPPLEMENTAL INFORMATION

Supplemental information can be found online at https://doi.org/10.1016/j.celrep.2021.110094.

ACKNOWLEDGMENTS

M.D.F. and P.C. received funding from Fondazione Italiana Sclerosi Multipla (FISM; project codes 2010/R/10, 2011/R/10, and 2013/R/12). M.D.F. also received support from the Ministero della Salute—Ricerca Finalizzata—Bando Giovani Ricercatori (project code GR-2010-2312924), from Fondo Ricerca di Base 2020 (University of Perugia), and from the Oak Foundation. A. Megaro received support from Regione Umbria. All the authors thank Gisella Guerrera and Francesca Gargano (Neuroimmunology Unit, IRCCS Fondazione Santa Lucia, Rome) for their contribution to the analysis of the potential clinical implications of the study. This work is dedicated to the memory of Dr. Emanuele Mattucci.

AUTHOR CONTRIBUTIONS

M.D.F., A. Mancini, L.G., and P.C. conceived the study; L.B., M.T., V.D., P.M., A. Megaro, M.S., A. Mancini, and A.T. performed and interpreted the electrophysiological experiments; A. Mancini, L.B., M.S., A. Megaro, and A.T. performed and interpreted the behavioral experiments; T.Z., A.D.L., and L.R. provided the genetic murine models and performed ELISA measurements of IL-17A levels; D.C. contributed to measurements of IL-17A levels; M.T.V. and L.L.B. performed and interpreted the morphological and western blot experiments and prepared the corresponding figures; N.S., V.L., L.P., E.P., and M.P.A. contributed to the interpretation of the results; A. Mancini, L.B., and L.G. prepared the draft of the manuscript and the figures; all the authors interpreted the experimental results and reviewed the final draft of the manuscript.

DECLARATION OF INTERESTS

M.D.F. participated on advisory boards for and received speaker or writing honoraria and funding for traveling from Bayer, Biogen Idec, Genzyme, Merck, Mylan, Novartis, Roche, and Teva. A. Mancini received speaker or writing honoraria and travel grants to attend national and international conferences from Almirall, Biogen Idec, Merck, Mylan, Novartis, Sanofi, and Teva. L.G. participated on advisory boards for and received speaker or writing honoraria and funding for traveling from Almirall, Biogen, Biogen-Idec, Genzyme, Mylan, Novartis, Roche, and Teva. E.P. served on scientific advisory board for Biogen Idec and Merck Serono and received honoraria for speaking and funding for traveling from Biogen, Genzyme, Novartis, Merck, and Teva. M.P.A. participated on advisory boards for and received speaker honoraria and research funding from Bayer, Biogen Idec, Sanofi Genzyme, Merck, Novartis, Roche, and Teva. P.C. received/receives research support from Bayer Schering, Biogen-Dompé, Boehringer Ingelheim, Eisai, Lundbeck, Merck-Serono, Novartis, Sanofi-Aventis, Sigma-Tau, and UCB Pharma. P.M., T.Z., A.L., M.T., A. Megaro, L.B., M.S., A.T., V.D., D.C., N.S., V.L., C.C., L.P., M.T.V., L.L.B., P.S., and L.R. declare no competing interests.

Received: May 26, 2020
Revised: August 6, 2021
Accepted: November 12, 2021
Published: December 7, 2021

REFERENCES

Amor, S., Smith, P.A., Hart, B., and Baker, D. (2005). Biozzi mice: of mice and human neurological diseases. J. Neuroimmunol. *165*, 1–10.

Asok, A., Leroy, F., Rayman, J.B., and Kandel, E.R. (2019). Molecular Mechanisms of the Memory Trace. Trends Neurosci. *42*, 14–22.

Bergsland, N., Zivadinov, R., Dwyer, M.G., Weinstock-Guttman, B., and Benedict, R.H.B. (2016). Localized atrophy of the thalamus and slowed cognitive processing speed in MS patients. Mult. Scler. *22*, 1327–1336.

Calabrese, M., Agosta, F., Rinaldi, F., Mattisi, I., Grossi, P., Favaretto, A., Atzori, M., Bernardi, V., Barachino, L., Rinaldi, L., et al. (2009). Cortical lesions and atrophy associated with cognitive impairment in relapsing-remitting multiple sclerosis. Arch. Neurol. *66*, 1144–1150.

Chen, C., Itakura, E., Nelson, G.M., Sheng, M., Laurent, P., Fenk, L.A., Butcher, R.A., Hegde, R.S., and de Bono, M. (2017). IL-17 is a neuromodulator of Caenorhabditis elegans sensory responses. Nature *542*, 43–48.

Cocozza, S., Petracca, M., Mormina, E., Buyukturkoglu, K., Podranski, K., Heinig, M.M., Pontillo, G., Russo, C., Tedeschi, E., Russo, C.V., et al. (2017). Cerebellar lobule atrophy and disability in progressive MS. J. Neurol. Neurosurg. Psychiatry *88*, 1065–1072.

Cryan, J.F., and Dinan, T.G. (2012). Mind-altering microorganisms: the impact of the gut microbiota on brain and behaviour. Nat. Rev. Neurosci. *13*, 701–712.

Dantzer, R., O'Connor, J.C., Freund, G.G., Johnson, R.W., and Kelley, K.W. (2008). From inflammation to sickness and depression: when the immune system subjugates the brain. Nat. Rev. Neurosci. *9*, 46–56.

DeLuca, G.C., Yates, R.L., Beale, H., and Morrow, S.A. (2015). Cognitive impairment in multiple sclerosis: clinical, radiologic and pathologic insights. Brain Pathol. *25*, 79–98.

Di Filippo, M., Sarchielli, P., Picconi, B., and Calabresi, P. (2008). Neuroinflammation and synaptic plasticity: theoretical basis for a novel, immune-centred, therapeutic approach to neurological disorders. Trends Pharmacol. Sci. *29*, 402–412.

Di Filippo, M., Chiasserini, D., Gardoni, F., Viviani, B., Tozzi, A., Giampà, C., Costa, C., Tantucci, M., Zianni, E., Boraso, M., et al. (2013). Effects of central and peripheral inflammation on hippocampal synaptic plasticity. Neurobiol. Dis. *52*, 229–236.

Di Filippo, M., de Iure, A., Durante, V., Gaetani, L., Mancini, A., Sarchielli, P., and Calabresi, P. (2015). Synaptic plasticity and experimental autoimmune encephalomyelitis: implications for multiple sclerosis. Brain Res. *1621*, 205–213.

Di Filippo, M., de Iure, A., Giampà, C., Chiasserini, D., Tozzi, A., Orvietani, P.L., Ghiglieri, V., Tantucci, M., Durante, V., Quiroga-Varela, A., et al. (2016). Persistent activation of microglia and NADPH oxidase [corrected] drive hippocampal dysfunction in experimental multiple sclerosis. Sci. Rep. *6*, 20926.

Di Filippo, M., Portaccio, E., Mancini, A., and Calabresi, P. (2018). Multiple sclerosis and cognition: synaptic failure and network dysfunction. Nat. Rev. Neurosci. *19*, 599–609.

Dineen, R.A., Vilisaar, J., Hlinka, J., Bradshaw, C.M., Morgan, P.S., Constantinescu, C.S., and Auer, D.P. (2009). Disconnection as a mechanism for cognitive dysfunction in multiple sclerosis. Brain *132*, 239–249.

Dutra, R.C., Moreira, E.L.G., Alberti, T.B., Marcon, R., Prediger, R.D., and Calixto, J.B. (2013). Spatial reference memory deficits precede motor dysfunction in an experimental autoimmune encephalomyelitis model: the role of kallikrein-kinin system. Brain Behav. Immun. *33*, 90–101.

Ely, L.K., Fischer, S., and Garcia, K.C. (2009). Structural basis of receptor sharing by interleukin 17 cytokines. Nat. Immunol. *10*, 1245–1251.

Fleming, C., Cai, Y., Sun, X., Jala, V.R., Xue, F., Morrissey, S., Wei, Y.L., Chien, Y.H., Zhang, H.G., Haribabu, B., et al. (2017). Microbiota-activated $CD103^{+}$ DCs stemming from microbiota adaptation specifically drive $\gamma\delta$T17 proliferation and activation. Microbiome *5*, 46.

Haak, S., Croxford, A.L., Kreymborg, K., Heppner, F.L., Pouly, S., Becher, B., and Waisman, A. (2008). IL-17A and IL-17F do not contribute vitally to autoimmune neuro-inflammation in mice. J. Clin. Invest. *119*, 61–69.

Haji, N., Mandolesi, G., Gentile, A., Sacchetti, L., Fresegna, D., Rossi, S., Musella, A., Sepman, H., Motta, C., Studer, V., et al. (2012). TNF-α-mediated anxiety in a mouse model of multiple sclerosis. Exp. Neurol. *237*, 296–303.

Harrison, D.M., Roy, S., Oh, J., Izbudak, I., Pham, D., Courtney, S., Caffo, B., Jones, C.K., van Zijl, P., and Calabresi, P.A. (2015). Association of Cortical Lesion Burden on 7-T Magnetic Resonance Imaging With Cognition and Disability in Multiple Sclerosis. JAMA Neurol. *72*, 1004–1012.

Hulst, H.E., Schoonheim, M.M., Van Geest, Q., Uitdehaag, B.M.J., Barkhof, F., and Geurts, J.J.G. (2015). Memory impairment in multiple sclerosis: Relevance of hippocampal activation and hippocampal connectivity. Mult. Scler. *21*, 1705–1712.

Kawanokuchi, J., Shimizu, K., Nitta, A., Yamada, K., Mizuno, T., Takeuchi, H., and Suzumura, A. (2008). Production and functions of IL-17 in microglia. J. Neuroimmunol. *194*, 54–61.

Kim, D.Y., Hao, J., Liu, R., Turner, G., Shi, F.D., and Rho, J.M. (2012). Inflammation-mediated memory dysfunction and effects of a ketogenic diet in a murine model of multiple sclerosis. PLoS One *7*, e35476.

Komiyama, Y., Nakae, S., Matsuki, T., Nambu, A., Ishigame, H., Kakuta, S., Sudo, K., and Iwakura, Y. (2006). IL-17 Plays an Important Role in the Development of Experimental Autoimmune Encephalomyelitis. J. Immunol. *177*, 566–573.

Lemon, N., and Manahan-Vaughan, D. (2006). Dopamine D1/D5 receptors gate the acquisition of novel information through hippocampal long-term potentiation and long-term depression. J. Neurosci. *26*, 7723–7729.

Li, X., Bechara, R., Zhao, J., McGeachy, M.J., and Gaffen, S.L. (2019). IL-17 receptor-based signaling and implications for disease. Nat. Immunol. *20*, 1594–1602.

Liu, Q., Xin, W., He, P., Turner, D., Yin, J., Gan, Y., Shi, F.-D., and Wu, J. (2014). Interleukin-17 inhibits adult hippocampal neurogenesis. Sci. Rep. *4*, 7554.

Lv, M., Liu, Y., Zhang, J., Sun, L., Liu, Z., Zhang, S., Wang, B., Su, D., and Su, Z. (2011). Roles of inflammation response in microglia cell through Toll-like receptors 2/interleukin-23/interleukin-17 pathway in cerebral ischemia/reperfusion injury. Neuroscience *176*, 162–172.

McGinley, A.M., Sutton, C.E., Edwards, S.C., Leane, C.M., DeCourcey, J., Teijeiro, A., Hamilton, J.A., Boon, L., Djouder, N., and Mills, K.H.G. (2020). Interleukin-17A Serves a Priming Role in Autoimmunity by Recruiting IL-1β-Producing Myeloid Cells that Promote Pathogenic T Cells. Immunity *52*, 342–356.e6.

Mori, F., Kusayanagi, H., Buttari, F., Centini, B., Monteleone, F., Nicoletti, C.G., Bernardi, G., Di Cantogno, E.V., Marciani, M.G., and Centonze, D. (2012). Early treatment with high-dose interferon beta-1a reverses cognitive and cortical plasticity deficits in multiple sclerosis. Funct. Neurol. *27*, 163–168.

Moynes, D.M., Vanner, S.J., and Lomax, A.E. (2014). Participation of interleukin 17A in neuroimmune interactions. Brain Behav. Immun. *41*, 1–9.

Murphy, A.C., Lalor, S.J., Lynch, M.A., and Mills, K.H.G. (2010). Infiltration of Th1 and Th17 cells and activation of microglia in the CNS during the course of experimental autoimmune encephalomyelitis. Brain Behav. Immun. *24*, 641–651.

Nicoll, R.A. (2017). A Brief History of Long-Term Potentiation. Neuron *93*, 281–290.

Olechowski, C.J., Tenorio, G., Sauve, Y., and Kerr, B.J. (2013). Changes in nociceptive sensitivity and object recognition in experimental autoimmune encephalomyelitis (EAE). Exp. Neurol. *241*, 113–121.

Planche, V., Koubiyr, I., Romero, J.E., Manjon, J.V., Coupé, P., Deloire, M., Dousset, V., Brochet, B., Ruet, A., and Tourdias, T. (2018). Regional hippocampal vulnerability in early multiple sclerosis: Dynamic pathological spreading from dentate gyrus to CA1. Hum. Brain Mapp. *39*, 1814–1824.

Preziosa, P., Rocca, M.A., Pagani, E., Stromillo, M.L., Enzinger, C., Gallo, A., Hulst, H.E., Atzori, M., Pareto, D., Riccitelli, G.C., et al.; MAGNIMS Study Group (2016). Structural MRI correlates of cognitive impairment in patients with multiple sclerosis: A Multicenter Study. Hum. Brain Mapp. *37*, 1627–1644.

Reed, M.D., Yim, Y.S., Wimmer, R.D., Kim, H., Ryu, C., Welch, G.M., Andina, M., King, H.O., Waisman, A., Halassa, M.M., et al. (2020). IL-17a promotes sociability in mouse models of neurodevelopmental disorders. Nature *577*, 249–253.

Reich, D.S., Lucchinetti, C.F., and Calabresi, P.A. (2018). Multiple Sclerosis. N. Engl. J. Med. *378*, 169–180.

Ribeiro, M., Brigas, H.C., Temido-Ferreira, M., Pousinha, P.A., Regen, T., Santa, C., Coelho, J.E., Marques-Morgado, I., Valente, C.A., Omenetti, S., et al. (2019). Meningeal $\gamma\delta$ T cell-derived IL-17 controls synaptic plasticity and short-term memory. Sci. Immunol. *4*, eaay5199.

Rocca, M.A., Amato, M.P., De Stefano, N., Enzinger, C., Geurts, J.J., Penner, I.-K., Rovira, A., Sumowski, J.F., Valsasina, P., and Filippi, M.; MAGNIMS Study Group (2015). Clinical and imaging assessment of cognitive dysfunction in multiple sclerosis. Lancet Neurol. *14*, 302–317.

Rostami, A., and Ciric, B. (2013). Role of Th17 cells in the pathogenesis of CNS inflammatory demyelination. J. Neurol. Sci. *333*, 76–87.

Schneider, H., Pitossi, F., Balschun, D., Wagner, A., del Rey, A., and Besedovsky, H.O. (1998). A neuromodulatory role of interleukin-1beta in the hippocampus. Proc. Natl. Acad. Sci. USA *95*, 7778–7783.

Sgobio, C., Ghiglieri, V., Costa, C., Bagetta, V., Siliquini, S., Barone, I., Di Filippo, M., Gardoni, F., Gundelfinger, E.D., Di Luca, M., et al. (2010). Hippocampal synaptic plasticity, memory, and epilepsy: effects of long-term valproic acid treatment. Biol. Psychiatry *67*, 567–574.

Steenwijk, M.D., Geurts, J.J.G., Daams, M., Tijms, B.M., Wink, A.M., Balk, L.J., Tewarie, P.K., Uitdehaag, B.M.J., Barkhof, F., Vrenken, H., and Pouwels, P.J. (2016). Cortical atrophy patterns in multiple sclerosis are non-random and clinically relevant. Brain *139*, 115–126.

Titley, H.K., Brunel, N., and Hansel, C. (2017). Toward a Neurocentric View of Learning. Neuron *95*, 19–32.

Trenova, A.G., Slavov, G.S., Draganova-Filipova, M.N., Mateva, N.G., Manova, M.G., Miteva, L.D., and Stanilova, S.A. (2018). Circulating levels of interleukin-17A, tumor necrosis factor-alpha, interleukin-18, interleukin-10, and cognitive performance of patients with relapsing-remitting multiple sclerosis. Neurol. Res. *40*, 153–159.

Tzartos, J.S., Friese, M.A., Craner, M.J., Palace, J., Newcombe, J., Esiri, M.M., and Fugger, L. (2008). Interleukin-17 production in central nervous system-infiltrating T cells and glial cells is associated with active disease in multiple sclerosis. Am. J. Pathol. *172*, 146–155.

van den Berg, R., Laman, J.D., van Meurs, M., Hintzen, R.Q., and Hoogenraad, C.C. (2016). Rotarod motor performance and advanced spinal cord lesion image analysis refine assessment of neurodegeneration in experimental autoimmune encephalomyelitis. J. Neurosci. Methods *262*, 66–76.

Wagner, E.F., and Nebreda, A.R. (2009). Signal integration by JNK and p38 MAPK pathways in cancer development. Nat. Rev. Cancer *9*, 537–549.

Waisman, A., Hauptmann, J., and Regen, T. (2015). The role of IL-17 in CNS diseases. Acta Neuropathol. *129*, 625–637.

Wang, D.D., Zhao, Y.F., Wang, G.Y., Sun, B., Kong, Q.F., Zhao, K., Zhang, Y., Wang, J.H., Liu, Y.M., Mu, L.L., et al. (2009). IL-17 potentiates neuronal injury induced by oxygen-glucose deprivation and affects neuronal IL-17 receptor expression. J. Neuroimmunol. *212*, 17–25.

Xu, S., and Cao, X. (2010). Interleukin-17 and its expanding biological functions. Cell. Mol. Immunol. *7*, 164–174.

Zepp, J., Wu, L., and Li, X. (2011). IL-17 receptor signaling and T helper 17-mediated autoimmune demyelinating disease. Trends Immunol. *32*, 232–239.

STAR★METHODS

KEY RESOURCES TABLE

REAGENT or RESOURCE	SOURCE	IDENTIFIER
Antibodies		
Mouse anti-neuronal nuclei (NeuN)	Merk Millipore	Cat# MAB-377; RRID: AB_2298772
Rabbit anti-neuronal nuclei (NeuN)	Merk Millipore	Cat# ABN78; RRID: AB_10807945
Rabbit anti-IL-17RA	Abcam	Cat#ab180904; RRID: AB_2756838
Mouse anti-IL-17A	Santa Cruz Biotechnology	Cat# sc-374218; RRID: AB_10988239
Mouse anti-IL-17A	R&D Systems	Cat# MAB-721; RRID: AB_2125017
Mouse IgG_{2A} isotype control	R&D Systems	Cat# MAB-003; RRID: AB_357345
Rabbit anti-GFAP	Merk Millipore	Cat# AB5804; RRID: AB_2109645
Goat anti-GFAP	Abcam	Cat# ab53554; RRID: AB_880202
Mouse anti Iba-1	Santa Cruz Biotechnology	Cat# sc-32725; RRID: AB_667733
Goat anti Iba-1	Novusbio	Cat# NB100-1028; RRID: AB_521594
Rabbit anti p38 MAPK	Cell Signaling	Cat# 8690; RRID: AB_10999090
Mouse anti p-p38 MAPK (Tyr 182)	Santa Cruz Biotechnology	Cat #sc-166182; RRID: AB_2141746
Mouse anti-GAPDH	Calbiochem	Cat# CB1001; RRID: AB_2107426
Neuro-Trace®640/660 deep-red Fluorescent Nissl Stain	Invitrogen	Cat# N21483
Alexa Fluor donkey anti-goat 488	Invitrogen	Cat# A-11055; RRID: AB_2534102
Alexa Fluor donkey anti-rabbit 488	Invitrogen	Cat# A-21206; RRID: AB_2535792
Alexa Fluor donkey anti-mouse 555	Invitrogen	Cat# A-31570; RRID: AB_2536180
Alexa Fluor donkey anti-rabbit 555	Invitrogen	Cat# A-31572; RRID: AB_162543
Alexa Fluor donkey anti-mouse 647	Invitrogen	Cat# A-31571; RRID: AB_162542
Anti-mouse HRP	Cell Signaling	Cat# 7076; RRID: AB_330924
Anti-rabbit HRP	Cell Signaling	Cat# 7074; RRID: AB_2099233
Bacterial and virus strains		
M. Tuberculosis dessicated H37Ra	BD Difco laboratories	Cat# 231141
M. Butyricum dessicated	BD Difco laboratories	Cat# 264010
Biological samples		
Hippocampal brain slices	Mice brain dissection	N/A
Chemicals, peptides, and recombinant proteins		
Freund's adjuvant, incomplete	Sigma-Aldrich	Cat# F5506
Pertussis toxin from *Bordetella pertussis*	Sigma-Aldrich	Cat# P7208
Myelin oligodendrocyte glycoprotein 35-55 (MOG_{35-55})	Cambridge Research Biochemicals	Cat# crb1000205n
Recombinant mouse IL-17A	R&D Systems	Cat# 421-ML
DAPI	Sigma-Aldrich	Cat# D9542
SB 202190	Tocris Biosciences	Cat# 1264
Critical commercial assays		
Mouse IL-17A ELISA assays	Duoset R&D system	Cat# DY421
Experimental models: Organisms/strains		
Biozzi ABH mice	Internal breeding	N/A
Wild-type C57BL/6 mice	Charles River Laboratories	Cat# 027C57BL/6
Genetic murine model lacking IL-17A	Internal breeding	N/A
Genetic murine model lacking IL-17RA	Internal breeding	N/A
Software and algorithms		
AxonpCLAMP Electrophysiology Data Acquisition	https://www.moleculardevices.com	Version 10
Graphpad Prism	https://www.graphpad.com	Version 7

(*Continued on next page*)

Continued

REAGENT or RESOURCE	SOURCE	IDENTIFIER
CorelDRAW	https://www.coreldraw.com/en/	2021
ImageJ software	National Institutes of Health, Bethesda, MD, USA	https://rsb.info.nih.gov/ij/
iBright Imaging System	Thermo Fisher Scientific	CL750
Other		
Axoclamp amplifier	Axon Instruments	2B
Digidata	Axon Instruments	1440A
Microplate reader	TECAN	Infinite M200
Confocal mycroscopy	ZEISS	LSM 800
Differential interference contrast (Nomarski) and infrared microscopy	Olympus	BX51WI

RESOURCE AVAILABILITY

Lead contact

Further information and requests for resources and reagents should be directed to and will be fulfilled by the Lead Contact, Professor Massimiliano Di Filippo (massimiliano.difilippo@unipg.it).

Materials availability

This study did not generate new unique reagents.

Data and code availability

- All data reported in this paper will be shared by the lead contact upon request.
- This paper does not report original code.
- Any additional information required to reanalyze the data reported in this paper is available from the lead contact upon request.

EXPERIMENTAL MODEL AND SUBJECT DETAILS

Animals and induction of experimental autoimmune encephalomyelitis

Six to eight-week-old male Biozzi ABH mice, wild-type C57BL/6 mice and genetic murine models lacking IL-17A (IL-17A$^{-/-}$) or IL-17RA (IL-17RA$^{-/-}$) obtained from the same genetic C57BL/6 background, were utilized for the electrophysiological recordings (wild-type littermates have been used as controls for all the protocols involving mice lacking IL-17A or IL-17RA). A co-housing equilibration of at least 4 weeks was applied before experiments. All procedures involving animals were performed in conformity with the European Directive 2010/63/EU, in accordance with protocols approved by the Animal Care and Use Committee at the University of Perugia. Chronic-relapsing experimental autoimmune encephalomyelitis (crEAE in the main text) was chosen as experimental model of MS for the electrophysiological and biochemical protocols assessing the acute and recovery phases of the disease, since it predictably follows a clinical course reminiscent of human MS with an acute phase followed by clinical remission (Amor et al., 2005). crEAE was induced as previously described (Di Filippo et al., 2013, 2016). MOG$_{35-55}$-induced EAE (EAE in the main text) was chosen as experimental model of MS for the behavioral experiments involving mice lacking IL-17A (IL-17A$^{-/-}$) obtained from C57BL/6 background. EAE was induced through the subcutaneous inoculation of 200 μg MOG$_{35-55}$ emulsified in Freund's incomplete adjuvant, supplemented with 8 mg/ml *M. tuberculosis H37Ra* at day 0. Mice were also intra-peritoneally injected with 500 ng of Pertussis toxin at day 0 and day 2. In both the crEAE and EAE groups, animals were monitored and weighed daily, from day 10 post-inoculation (p.i.) onward, to assess the development of relapsing-remitting paralysis. All efforts were made to minimize the number of animals used and their suffering.

METHOD DETAILS

Electrophysiology

For hippocampal recordings mice were sacrificed by cervical dislocation. The brain was dissected and immersed in ice-cold artificial cerebrospinal fluid (ACSF) containing (in mM): 126 NaCl, 2.5 KCl, 1.2 $MgCl_2$, 1.2 NaH_2PO_4, 2.4 $CaCl_2$, 10 glucose, and 25 $NaHCO_3$, continuously bubbled with 95% O_2 and 5% CO_2, pH 7.4. Transverse hippocampal slices (400 μm thickness for extracellular recording, 250 μm thickness for patch-clamp recordings) were cut by using a vibratome and were allowed to recover in oxygenated ACSF at 30°C for 30 minutes, and then at room temperature for another 1–2 hours before experimental recordings. Each slice was

then transferred into the recording chamber and submerged in ACSF at a constant rate of 2.9–3 mL/min at a temperature of 29°C. During electrophysiological experiments, drugs were bath applied by switching the flowing solution to ACSF containing known concentrations of each compound. Total replacement of the medium in the chamber occurred within 1 min. Experiments with exposure to IL-17A (alone or together with SB 202190), to anti-IL-17A Ab (R&D Systems, Cat# MAB-721; RRID: AB_2125017), or to mouse IgG_{2A} isotype control (R&D Systems, Cat# MAB-003; RRID: AB_357345) were performed through a pre-incubation of brain slices lasting 1 h before electrophysiological recordings. Under visual control, stimulating electrodes were inserted into the Schaffer collateral fibers, and a recording electrode into the CA1 region of the hippocampal slice. Whole-cell patch clamp recordings (holding potential, −60 mV) were performed with borosilicate glass pipettes filled with an intracellular solution containing (in mM): 145 K-gluconate, 0.1 $CaCl_2$, 2 $MgCl_2$, 0.1 EGTA, 10 HEPES, and 0.3 GTP, adjusted to pH 7.3 with KOH. Neurons of the CA1 region were visualized using differential interference contrast (Nomarski) and infrared microscopy (Olympus). Excitatory postsynaptic currents (EPSCs) of half-maximal amplitude were evoked every 10 s. For extracellular recordings, the stimulating electrodes were located under visual control into the Schaffer collaterals and the recording electrode into the hippocampal area CA1 (Di Filippo et al., 2013; Sgobio et al., 2010). Hippocampal field excitatory postsynaptic potentials (fEPSPs) were filtered at 3 KHz and digitized at 10 KHz using an Axoclamp 2B amplifier (Axon Instruments, USA). LTP was induced by high frequency stimulation (HFS) consisting of one train of one second at 100 Hz at a stimulus strength corresponding to 70% of maximum response (Sgobio et al., 2010), or through theta-burst stimulation (TBS) protocol (consisting of 10 consecutive trains with four pulses at 100 Hz separated by 200 ms) (Ribeiro et al., 2019).

Measurement of hippocampal IL-17A levels

Mice were sacrificed by cervical dislocation and hippocampal tissues were prepared as previously described (Di Filippo et al., 2016). Hippocampal IL-17A levels were assessed at different time points during crEAE through ELISA assays (Duoset R&D system, Assay Range: 16-1000 pg/ml).

Immunofluorescence

For morphological analysis mice were sacrificed as described above. The brains were dissected and post-fixed in paraformaldehyde overnight at 4°C and then immersed in a 30% sucrose solution at 4°C. The brains were cut into 30 μm-thick coronal sections using a freezing microtome. In order to avoid staining variability, brain sections of control and acute crEAE mice were concomitantly incubated with the same cocktail of primary and secondary antibodies. Specifically, the sections selected for immunofluorescence were blocked with PB containing 10% normal donkey serum for 2h at RT and then incubated for 48 h in PB and 0.3% Triton X-100 with a mixture of primary antibodies including mouse anti-neuronal nuclei (NeuN; 1:200; Merk Millipore, Cat# MAB-377; RRID: AB_2298772), rabbit anti-neuronal nuclei (NeuN; 1:600; Merk Millipore, Cat#ABN78; RRID: AB_10807945), rabbit anti-IL-17RA (1:200, Abcam, Cat# ab180904; RRID: AB_2756838), mouse anti-IL-17A (1:200; Santa Cruz Biotechnology Cat# sc-374218; RRID: AB_10988239), rabbit anti-GFAP (1:500, Merk Millipore Cat# AB5804; RRID: AB_2109645), goat anti-GFAP (1:500, Cat# Abcam, ab53554; RRID: AB_880202), mouse anti Iba-1 (1:200, Santa Cruz Biotechnology, Cat# sc-32725; RRID: AB_667733), goat anti Iba-1 (1:700, Novusbio, Cat# NB100-1028; RRID: AB_521594), rabbit anti-phospho-p38 (1:400, Cell Signaling, Cat# 8690; RRID: AB_10999090). After 3 washes in PB, the sections were incubated with a mixture of Alexa Fluor 488- 555- and 647-conjugated secondary antibodies (1:200, Invitrogen, USA) for 2h at RT and sections were counterstained with Neuro-Trace® 640/660 deep-red Fluorescent Nissl Stain (1: 200; Invitrogen; Cat# N21483) or 4′,6-diamidino-2-phenylindole (DAPI) (Sigma) to determine the cytoarchitectonic area (CA1 hippocampal region) of interest. The specificity of immunostaining and primary antibodies (IL-17A and IL-17RA) was verified by omitting the primary antibodies. Furthermore, with regard to the IL-17RA, the specificity of the antibody was confirmed by performing immunofluorescence in mice lacking IL-17RA, showing no expression of the receptor (n = 4) (Figure S2A). The sections were rinsed, mounted, coverslipped and then examined using a confocal laser scanning microscope (Zeiss LSM800, Germany). The confocal image acquisitions were performed using consistent settings for laser power and detector gain.

Western blot

Hippocampal slices were homogenized in RIPA buffer (50 mM Tris-HCl pH 7.4, 150 mM NaCl, 1mM EDTA, 5mM MgCl2, 1% Triton x-100, 0.25% sodium-deoxycholate, 0,1% SDS) containing a mixture of protease and phosphatase inhibitors (Roche Diagnostics). Equal amount of protein was loaded and separated on 10% SDS-PAGE gels (Bio-Rad) and transferred to PVDF membranes (Millipore). The membranes were blocked with 5% BSA in Tris-buffered saline (pH 7.6) with 0.1% Tween-20 for 1h at RT, and incubated overnight at 4°C with primary antibodies, followed by HRP-conjugated secondary antibodies for 1h at RT. GAPDH antibody was probed as a loading control.

Hole-board behavioral test

The hole-board test was performed as previously described (Di Filippo et al., 2016). Cages were positioned in the experiment room 1 hour before the experimental session in order to allow animal acclimatization. In the first day, animals were allowed to explore the recording chamber for 10 minutes (habituation). The first session of the test took place 24 hours after habituation. A hole-board floor (28 × 28 × 2.5 cm, with 4 holes at each corner, 2 cm in diameter and 2.5 cm deep) was positioned into the recording chamber and animals explored the new setting for 10 minutes (session 1) (Di Filippo et al., 2016). After 24 hours, animals explored the same experimental setting for 10 minutes (session 2) (Di Filippo et al., 2016). During both the sessions, the head-dipping into holes and the lo-

comotor activity were recorded. The box and the hole-boards were cleaned with alcohol (70%) and water solution after each trial (Di Filippo et al., 2016).

Drugs

Freund's incomplete adjuvant and Pertussis toxin were purchased from Sigma-Aldrich (Milan, Italy); myelin oligodendrocyte glycoprotein 35-55 (MOG_{35-55}) was purchased from Cambridge Research Biochemicals; desiccated mycobacteria, *M. tuberculosis H37Ra* and *M. butyricum*, were obtained from Difco laboratories (Detroit, U.S.A.); recombinant mouse IL-17A, mouse anti-IL-17A monoclonal Ab (Cat# MAB-721; RRID: AB_2125017) and mouse IgG_{2A} isotype control (Cat# MAB-003; RRID: AB_357345) were purchased from R&D Systems (Minneapolis, U.S.A.); SB 202190 was purchased from Tocris Biosciences (Bristol, UK). For immunofluorescence and confocal microscopy analysis were used the following antibodies: mouse anti-neuronal nuclei (NeuN; 1:200; Merk Millipore, Cat# MAB-377; RRID:AB_2298772), rabbit anti-IL-17RA (1:200, Abcam, Cat# ab180904; RRID:AB_2756838), mouse anti-IL-17A (1:200; Santa Cruz Biotechnology Cat# sc-374218; RRID:AB_10988239), rabbit anti-GFAP (1:500, Merk Millipore, Cat# AB5804; RRID:AB_2109645), goat anti-GFAP (1:500, Abcam, Cat# ab53554; RRID:AB_880202), mouse anti Iba-1 (1:200, Santa Cruz Biotechnology, Cat# sc-32725; RRID:AB_667733); anti p38MAPK (1:500; Cell Signaling: Cat# 8690; RRID:AB_10999090). For western blot analysis the following antibodies were used: p-p38 (Tyr 182; 1:500; Santa Cruz: Cat# sc-166182; RRID:AB_2141746), p38 (1:500; Cell Signaling: Cat# 8690; RRID:AB_10999090), GAPDH (1:5000; Calbiochem: Cat# CB1001; RRID:AB_2107426).

QUANTIFICATION AND STATISTICAL ANALYSIS

Clinical scoring of experimental autoimmune encephalomyelitis

Clinical signs of the experimental disease were scored as follows: 0 = normal; 1 = fully flaccid tail; 2 = impaired righting reflex; 3 = hind limb paresis; 4 = complete hindlimb paresis; 5 = moribund/death (Di Filippo et al., 2013, 2016). In order to investigate the pathogenic process associated with the experimental disease at different time points, mice affected by crEAE were divided in two main groups. Mice affected by the first episode of neurological deficit, suggestive of CNS inflammation (clinical neurological score of at least 3, approximately at day 15-18 p.i.) have been included in the "acute crEAE" group while mice displaying complete resolution of a previously documented relapse (clinical neurological score of 0, > 30 days p.i) were included in the "recovery crEAE" group.

Electrophysiology

The amplitude of EPSCs or the slope of fEPSPs were used to assess changes in synaptic strength. Values are presented in the text and figures as the mean ± standard error of the mean (SEM), expressing the % change of EPSC amplitude or fEPSP slope with respect to baseline values, recorded 50 min after the HFS or TBS protocol. Comparisons between groups have been made through two-way ANOVA, considering all the time-course of the EPSC amplitude or fEPSP slope after the HFS or TBS protocol, with Bonferroni's test for post hoc comparisons. The significance level was established at $p < 0.05$.

Measurement of hippocampal IL-17A levels

All measurements were performed at least two times, following manufacturer instructions. Absorbance was measured using a TECAN microplate reader (Infinite M200). An independent samples t test was used to assess differences between groups. The significance level was established at $p < 0.05$.

Immunofluorescence

Quantification of the IL-17A and IL-17RA immunoreactivity in the CA1 region of control and acute crEAE mice was performed by densitometric analysis. All quantitative analyses were conducted blind to the animal's experimental group. After confocal acquisition, images were exported in TIFF and analyzed with the ImageJ software (https://rsb.info.nih.gov/ij/; National Institutes of Health, Bethesda, MD, USA). The background signal was determined in a non-stained area. The threshold was adjusted according to the background signal and kept constant between sections. IL-17A- or 17RA-associated signal was quantified by manually outlining the areas of interest. The mean signal intensity (F) of IL-17A and IL-17RA was performed on two squared frames (50 μm per side) pseudo-randomly distributed dorso-ventrally on five sections sampled to cover the rostro-caudal extent of the CA1 (10 samples per mouse). The F/A ratio defines the mean fluorescence of individual samples (F) normalized to total cellular surface (A). Accordingly, quantification was performed on five mice per group.

Western blot

Signals were visualized using enhanced chemiluminescence (ECL, Pierce), and captured by iBright CL750 Imaging System (Thermo Fisher Scientific). Statistical analysis was performed through Welch t test. The significance level was established at $p < 0.05$.

Hole-board behavioral test

The test was analyzed by an observer blind to the experimental group, evaluating the number of head-dips into holes and the locomotor activity (showed as the mean ± SEM number of crossings among four equal sized squares in which the arena was divided). ANOVA or independent samples t test were used to assess differences between groups. The significance level was established at $p < 0.05$.